

US Spine Simulation and Results

Rui Xu
MBP rotation
Sept 8-Oct 14

October 5, 2016

1 Introduction

This document will outline my ultrasound code and results. I have constructed a simple two-dimensional simulation using existing code from the k-wave package to construct a two-transistor system. I'll start with an overview of the k-wave code for my own understanding and benefit.

2 The k-wave Toolbox

2.1 Governing equations for acoustic propagation

The k-wave toolbox is used to simulate the propagation of pressure waves through media, which is described by a set of couple first-order partial differential equations or the wave equation, a second-order partial differential equation. K-wave uses the first order equation,

$$\frac{\partial \mathbf{u}}{\partial t} = -\frac{1}{\rho_0} \nabla p \quad (1)$$

$$\frac{\partial p}{\partial t} = -\rho_0 \nabla \cdot \mathbf{u} \quad (2)$$

$$p = c_0^2 \rho \quad (3)$$

where \mathbf{u} is particle velocity, p is acoustic pressure, ρ is acoustic density, ρ_0 is equilibrium acoustic density, and c_0 is the isentropic speed of sound. In words, the change in particle velocity is given by the pressure gradient, divided by equilibrium acoustic density. That is, particle velocity will increase in the direction down the pressure gradient, and this increase is inversely proportional to the equilibrium acoustic density. This is the equation of momentum conservation. The second equation states that the change in acoustic density is proportional to equilibrium particle density times the divergence of the particle velocity field (particle flux). This is the equation of mass conservation. Finally, we have the pressure - density relationship, where pressure is equal to the isentropic speed of sound ($c_0 = \sqrt{K_s/\rho_0}$, K_s is the isentropic bulk modulus, squared, times the density at that location).

This set of equations in this forms assumes that the medium is isotropic and quiescent. However, these equations must include additional terms if the medium is anisotropic and has absorbent properties, as shown in the following equations:

$$\frac{\partial \mathbf{u}}{\partial t} = -\frac{1}{\rho_0} \nabla p \quad (4)$$

$$\frac{\partial p}{\partial t} = -\rho_0 \nabla \cdot \mathbf{u} - \mathbf{u} \cdot \nabla \rho_0 \quad (5)$$

$$p = c_0^2(\rho + \mathbf{d} \cdot \nabla \rho_0 - \mathbf{L}\rho) \quad (6)$$

In this case, the momentum conservation equation remains the same. An additional term is present in the mass conservation equation to represent the additional mass transfer due to inhomogeneity in the equilibrium density profile of the medium (resulting in a non-zero gradient in ρ_0). The pressure-density relationship changes significantly, with the addition of the inner product of

acoustic particle displacement \mathbf{d} with the gradient of ρ_0 , as well as a linear integro-differential operator ‘ \mathbf{L} ’ that accounts for acoustic absorption α) and dispersion in a medium that follows a frequency power law ($\alpha = \alpha_0 \omega^y$). This operator is defined:

$$\mathbf{L} = \tau \frac{\partial}{\partial t} (-\nabla^2)^{\frac{y}{2}-1} + \eta (-\nabla^2)^{\frac{y+1}{2}-1} \quad (7)$$

where τ and η are the absorption and dispersion proportionality coefficients:

$$\tau = -2\alpha_0 c_0^{y-1}, \quad \eta = 2\alpha_0 c_0^y \tan\left(\frac{\pi y}{2}\right) \quad (8)$$

where α_0 is the power law prefactor and y is the power law exponent.

Acoustic wave propagation ceases to be linear in certain biological circumstances, and in this case the governing equations of the system must be modified with higher order terms. k-Wave includes two non-linear terms encompassed by a nonlinearity parameter B/A , which characterizes the contribution of finite-amplitude effects to sound speed. The governing equations are now:

$$\frac{\partial \mathbf{u}}{\partial t} = -\frac{1}{\rho_0} \nabla p \quad (9)$$

$$\frac{\partial p}{\partial t} = -(2\rho_0 + \rho_0) \nabla \cdot \mathbf{u} - \mathbf{u} \cdot \nabla \rho_0 \quad (10)$$

$$p = c_0^2 \left(\rho + \mathbf{d} \cdot \nabla \rho_0 + \frac{B}{2A} \frac{\rho^2}{\rho_0} - \mathbf{L}\rho \right) \quad (11)$$

We can generate acoustic waves in a medium by adding a force source term \mathbf{S}_F to the momentum conservation equation and a mass source term and a mass source term \mathbf{S}_M to the mass conservation equation.

2.2 Pseudospectral method

The k-wave toolbox uses a k -space pseudospectral method for the calculation of spatial derivatives, and then uses a finite difference scheme for temporal updates. For example, we can take the wave equation system for a simple homogeneous and lossless system,

$$\nabla^2 p(\mathbf{x}, t) - \frac{1}{c_0^2} \frac{\partial^2}{\partial t^2} p(\mathbf{x}, t) \quad (12)$$

and use a spatial Fourier transform to rewrite the equation in k -space where it has the form:

$$\frac{\partial^2}{\partial t^2} p(\mathbf{k}, t) = -(c_0 k)^2 p(\mathbf{k}, t) \quad (13)$$

and we can rewrite the temporal derivative as:

$$\frac{\partial^2}{\partial t^2} p(\mathbf{k}, t) = \frac{p(\mathbf{k}, t + \Delta t) - 2p(\mathbf{k}, t) + p(\mathbf{k}, t - \Delta t)}{\Delta t^2} = -(c_0 k)^2 p(\mathbf{k}, t) \quad (14)$$

This finite difference approximation scheme is subject to dispersion for large scale simulations, and this dispersion results in the accumulation of phase errors. However, we can replace the Δt^2 term by multiplying a corrective operator, the k -space operator, $\kappa^2 = \text{sinc}^2(c_{\text{ref}} k \Delta t / 2)$. This technique is described in the textbook ‘Nonstandard Finite Difference Models of Differential Equations’, [1]. Another approach k-wave uses to increase the stability and accuracy of the simulation is by using staggered spatial and temporal grids.

2.3 Discretized equations

The mass and momentum equations, written in discrete form and using the k-space pseudospectral method, have the following form:

$$\frac{\partial}{\partial \xi} p^n = \mathcal{F}^{-1} \left[i k_\xi \kappa e^{i k_\xi \Delta \xi / 2} \mathcal{F} [p^n] \right] \quad (15)$$

$$u_\xi^{n+\frac{1}{2}} = u_\xi^{n-\frac{1}{2}} - \frac{\Delta t}{\rho_0} \frac{\partial}{\partial \xi} p^n + \Delta t \mathbf{S}_{\mathbf{F}_\xi}^n \quad (16)$$

$$\frac{\partial}{\partial \xi} u_\xi^{n+\frac{1}{2}} = \mathcal{F}^{-1} \left[i k_\xi \kappa e^{-i k_\xi \Delta \xi / 2} \mathcal{F} [u_\xi^{n+\frac{1}{2}}] \right] \quad (17)$$

$$\rho_\xi^{n+1} = \rho_\xi^n - \Delta t \rho_0 \frac{\partial}{\partial \xi} u_\xi^{n+\frac{1}{2}} + \Delta t \mathbf{S}_{\mathbf{F}_\xi}^{n+\frac{1}{2}} \quad (18)$$

In the above, the first and third equations are spatial gradient calculations and the second and fourth equations are update steps. The symbol ξ represents cartesian coordinates for one to three dimensional systems, k_ξ represents wavenumber in the ξ direction and is discretized according to:

$$k_\xi = \left[-\frac{N_\xi}{2}, -\frac{N_\xi}{2} + 1, \dots, \frac{N_\xi}{2} - 1 \right] \frac{2\pi}{\Delta \xi N_\xi} \quad (19)$$

if N_ξ is even, or

$$k_\xi = \left[-\frac{N-1_\xi}{2}, -\frac{N-1_\xi}{2} + 1, \dots, \frac{N-1_\xi}{2} \right] \frac{2\pi}{\Delta \xi N_\xi} \quad (20)$$

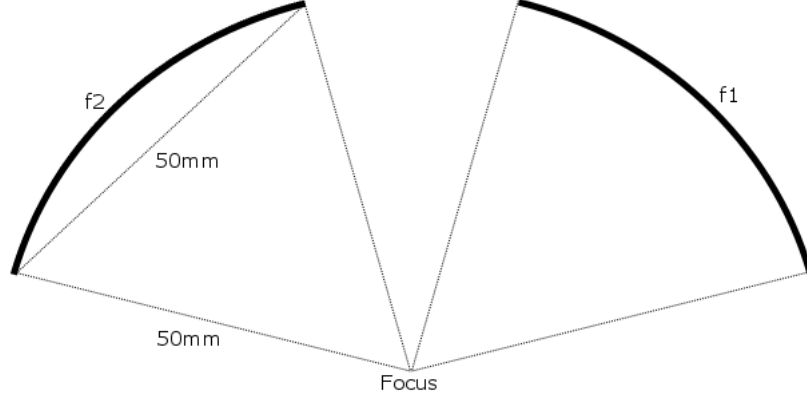
if N_ξ is odd. The algorithm follows a simple procedure, where pressure is known at timestep n , then pressure differentials are calculated at staggered grid points for this timestep n . Subsequently, particle velocity is calculated from these pressure differentials for timestep $n + 1/2$ at the staggered grid points. Next, velocity differentials are calculated at the regular grid points, and these velocity differentials are subsequently used to update density (and therefore pressure using the pressure-density relation) at the regular grid points for timestep $n + 1/2$. The discretized pressure-density relation is $p^{n+1} = c_0^2(\rho^{n+1} - \mathbf{L}_d)$, where \mathbf{L}_d is the discretized form of the power law absorption term (Equation 7). The discretized form of the power law absorption term is:

$$\mathbf{L}_d = \tau \mathcal{F}^{-1} \left[k^{y-2} \mathcal{F} \left[\frac{\partial}{\partial t} \rho^n \right] \right] + \eta \mathcal{F}^{-1} [k^{y-1} \mathcal{F} [\rho^{n+1}]] \quad (21)$$

$$= \tau \mathcal{F}^{-1} \left[k^{y-2} \mathcal{F} \left[\rho_0 \sum_\xi \frac{\partial}{\partial \xi} x_\xi^{n+\frac{1}{2}} \right] \right] + \eta \mathcal{F}^{-1} [k^{y-1} \mathcal{F} [\rho^{n+1}]] \quad (22)$$

3 System 1: Homogeneous Medium, Two Elements, Two Frequencies

The first system I created was a system of two curved transducers, each with a radius of curvature of 50mm, and each subtending $\pi/2$ radians. The two transducers are driven at frequencies f_1 and f_2 . The focal point of the two transducers are the same. I create the transducers by defining source points at a 50mm radius for $\pi/12 \leq \Theta_1 \leq 5\pi/12$ and $7\pi/12 \leq \Theta_2 \leq 11\pi/12$. The system setup is shown in Figure 3.



3.1 Half-Maximum Profiles

The first test was to vary the frequency f_1 of the right hand side transducer, while keeping the frequency of the second transducer constant $f_2 = 0.25\text{MHz}$. Implementing multiple frequencies in k-wave require that each source point have its frequency assigned to it. In the current implementation, then I've simply looped over all points, and set the frequency of the source points on the left half of the computational box to f_2 and those on the right half to f_1 . Take care with the current code if you move the transducers around. It may be advisable to write a foolproof version of the frequency assignment part of the code.

We are interested in the pressure profile of the system near the focal point, for different frequencies $0.15\text{MHz} \leq f_1 \leq 0.35\text{MHz}$, tested in increments of 10kHz. The following figures show the 2D root-mean-square pressure profiles. The points of half-maximum pressure are outlined in black.

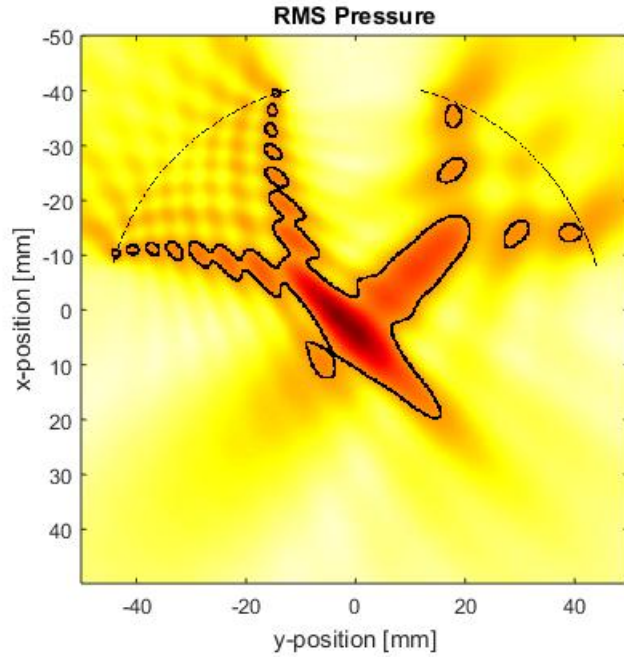


Figure 1: RMS pressure profile for $f_1 = 0.15\text{MHz}$, $f_2 = 0.25\text{MHz}$

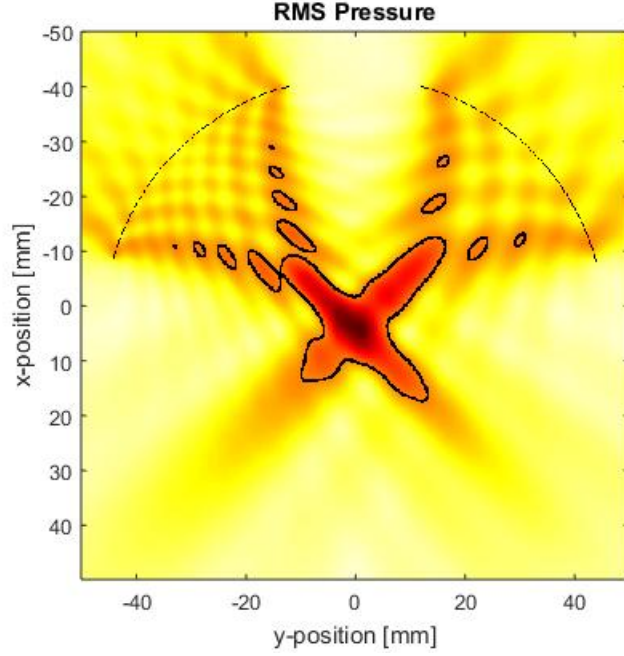


Figure 2: RMS pressure profile for $f_1 = 0.16\text{MHz}$, $f_2 = 0.25\text{MHz}$

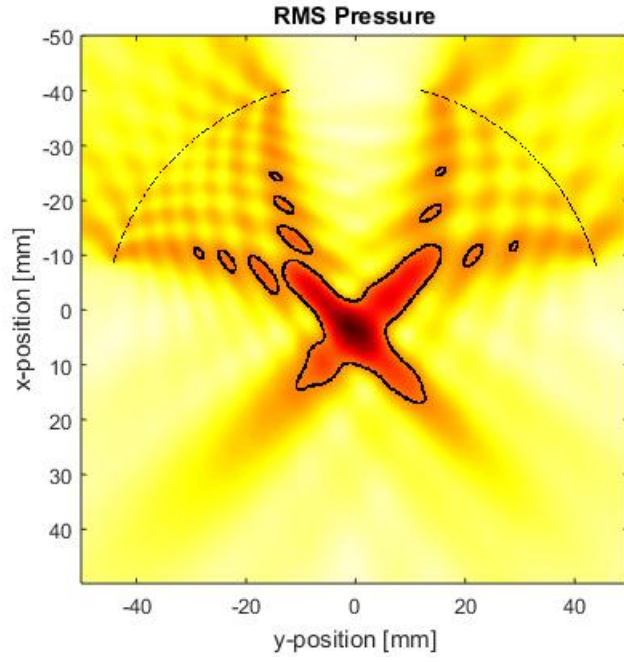


Figure 3: RMS pressure profile for $f_1 = 0.17\text{MHz}$, $f_2 = 0.25\text{MHz}$

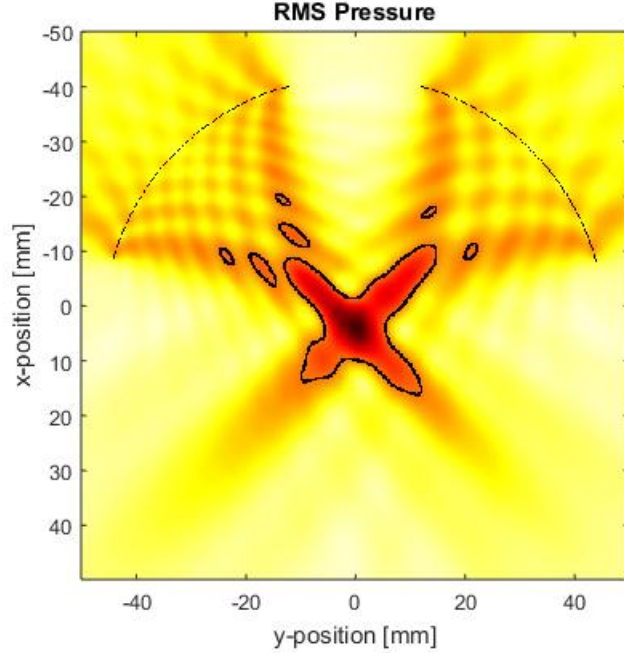


Figure 4: RMS pressure profile for $f_1 = 0.18\text{MHz}$, $f_2 = 0.25\text{MHz}$

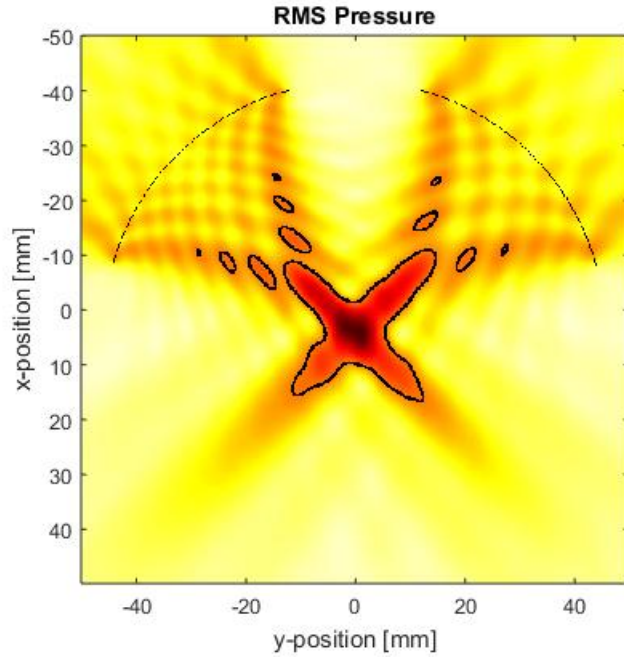


Figure 5: RMS pressure profile for $f_1 = 0.19\text{MHz}$, $f_2 = 0.25\text{MHz}$

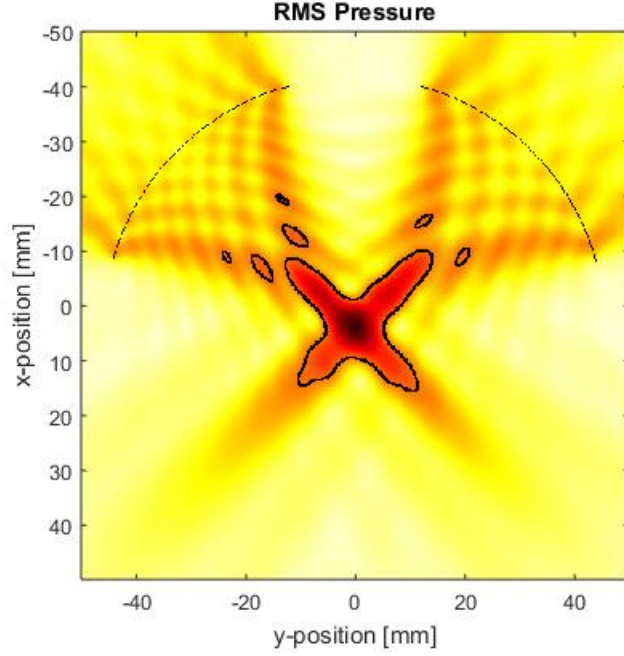


Figure 6: RMS pressure profile for $f_1 = 0.20\text{MHz}$, $f_2 = 0.25\text{MHz}$

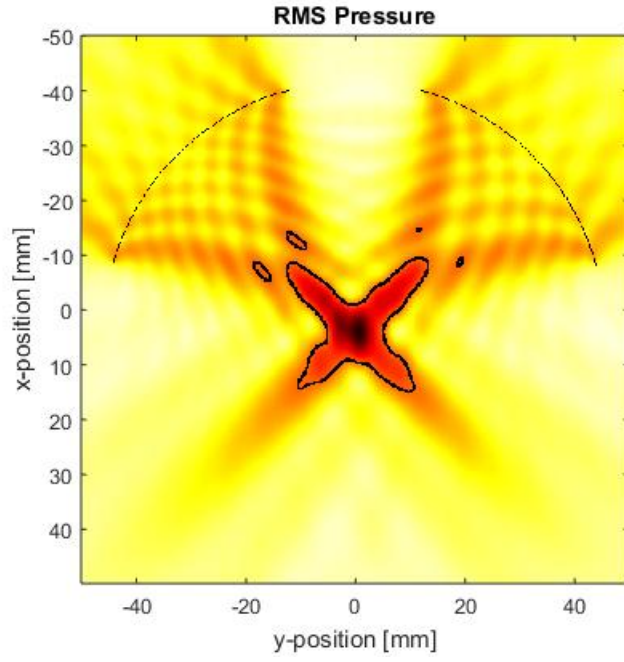


Figure 7: RMS pressure profile for $f_1 = 0.21\text{MHz}$, $f_2 = 0.25\text{MHz}$

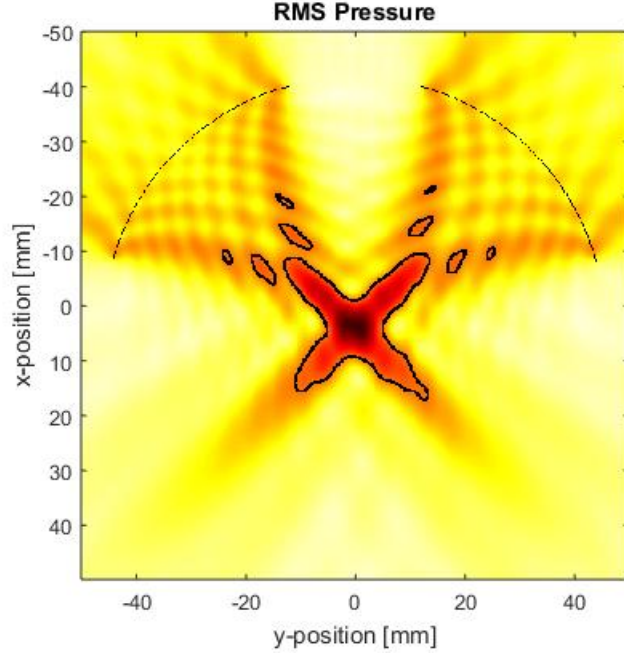


Figure 8: RMS pressure profile for $f_1 = 0.22\text{MHz}$, $f_2 = 0.25\text{MHz}$

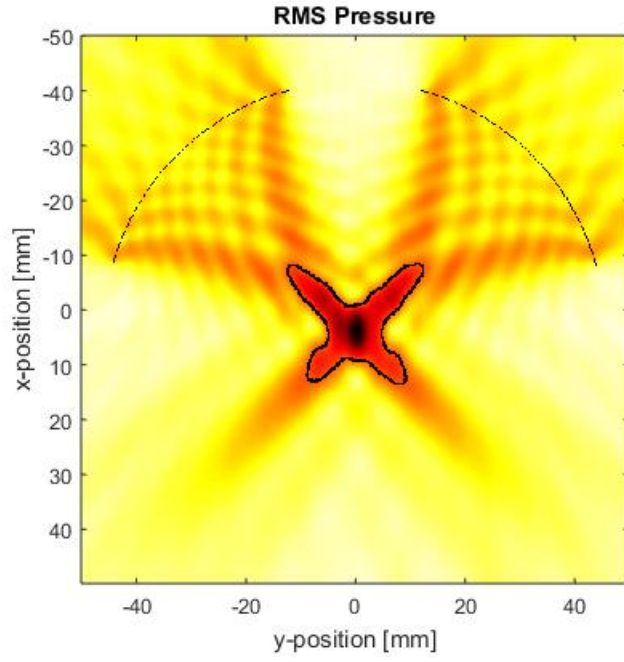


Figure 9: RMS pressure profile for $f_1 = 0.23\text{MHz}$, $f_2 = 0.25\text{MHz}$

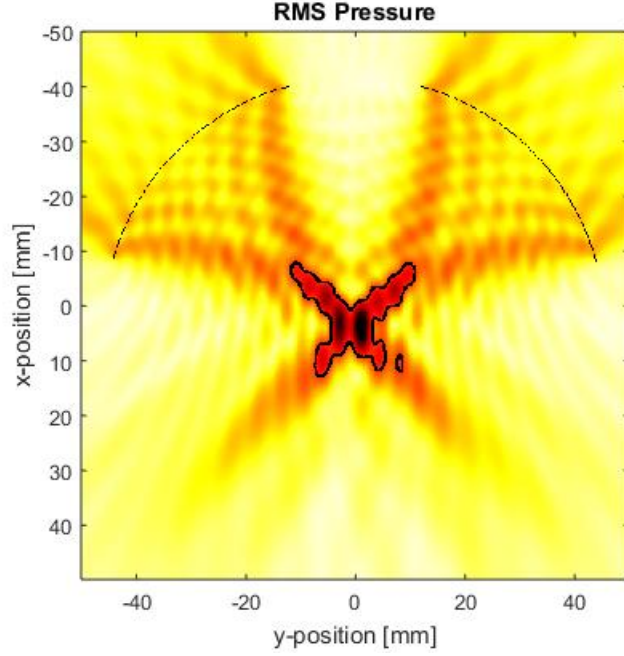


Figure 10: RMS pressure profile for $f_1 = 0.24\text{MHz}$, $f_2 = 0.25\text{MHz}$

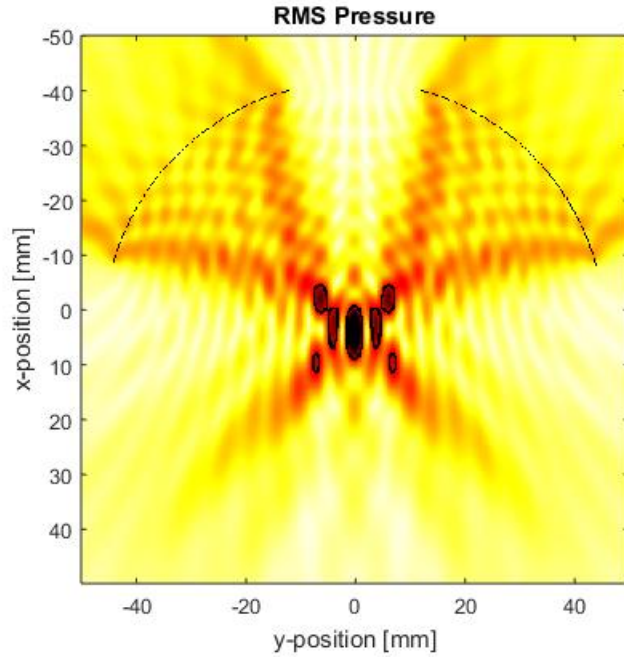


Figure 11: RMS pressure profile for $f_1 = 0.25\text{MHz}$, $f_2 = 0.25\text{MHz}$

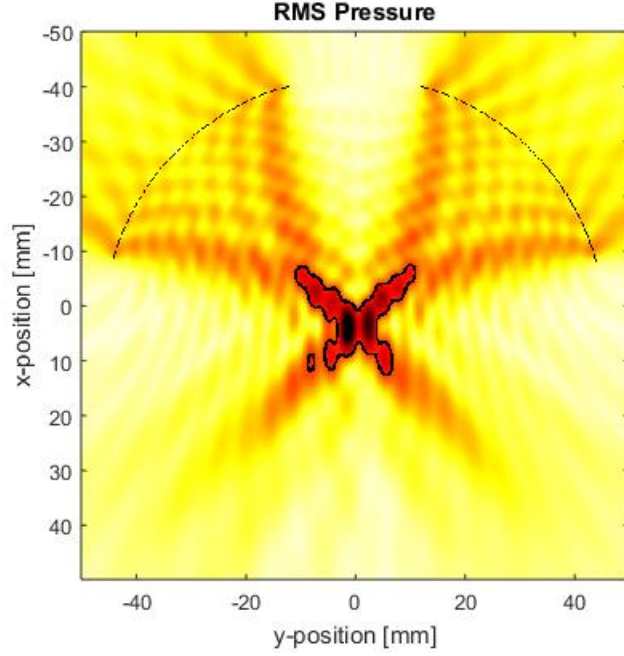


Figure 12: RMS pressure profile for $f_1 = 0.26\text{MHz}$, $f_2 = 0.25\text{MHz}$

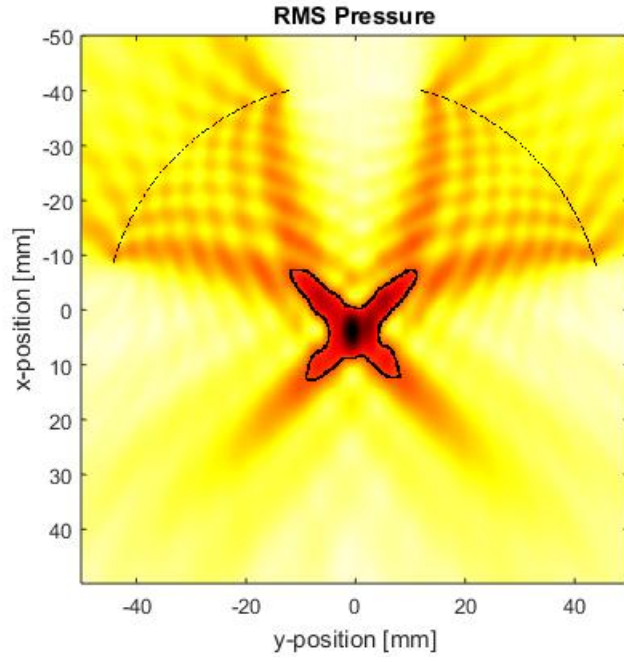


Figure 13: RMS pressure profile for $f_1 = 0.27\text{MHz}$, $f_2 = 0.25\text{MHz}$

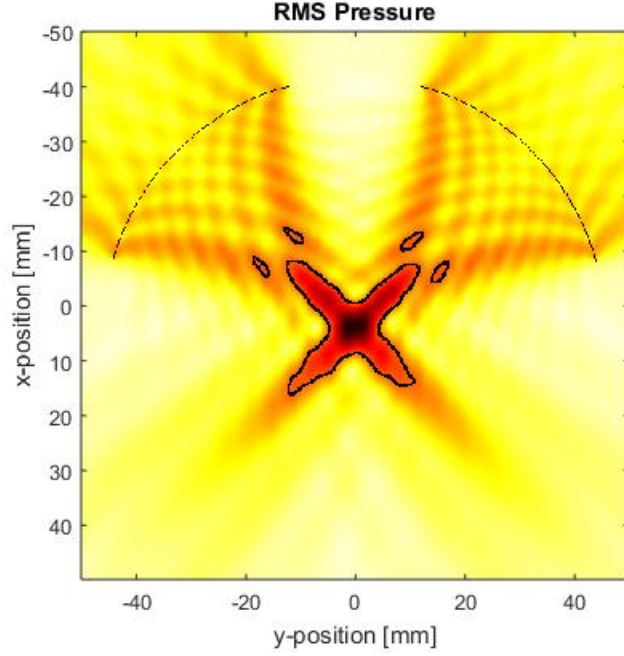


Figure 14: RMS pressure profile for $f_1 = 0.28\text{MHz}$, $f_2 = 0.25\text{MHz}$

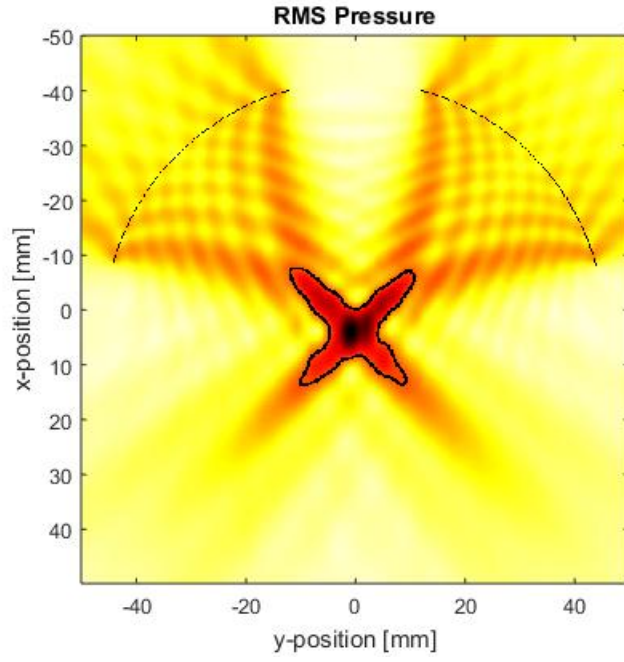


Figure 15: RMS pressure profile for $f_1 = 0.29\text{MHz}$, $f_2 = 0.25\text{MHz}$

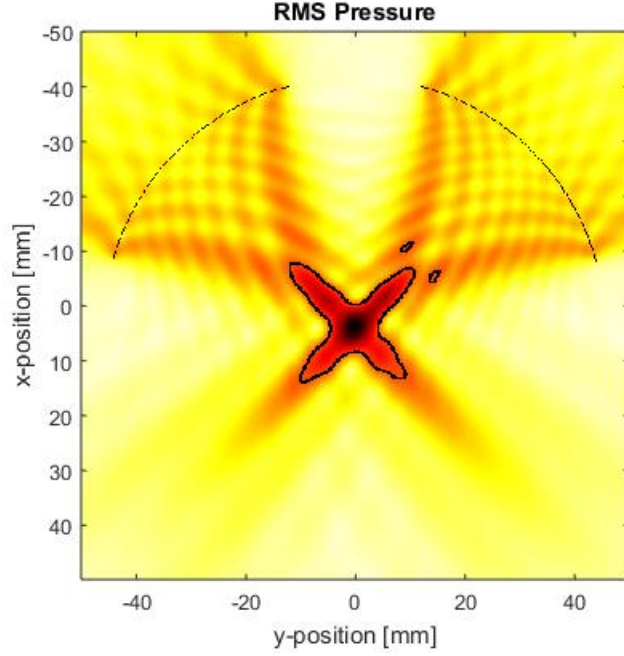


Figure 16: RMS pressure profile for $f_1 = 0.30\text{MHz}$, $f_2 = 0.25\text{MHz}$

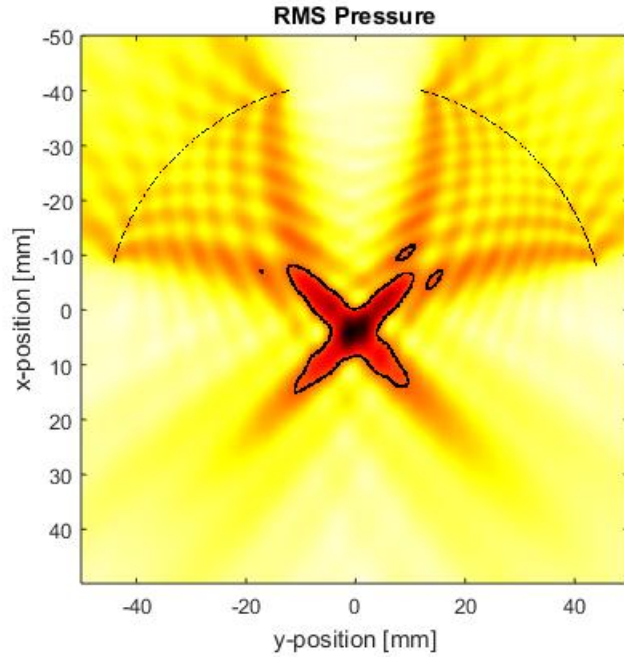


Figure 17: RMS pressure profile for $f_1 = 0.31\text{MHz}$, $f_2 = 0.25\text{MHz}$

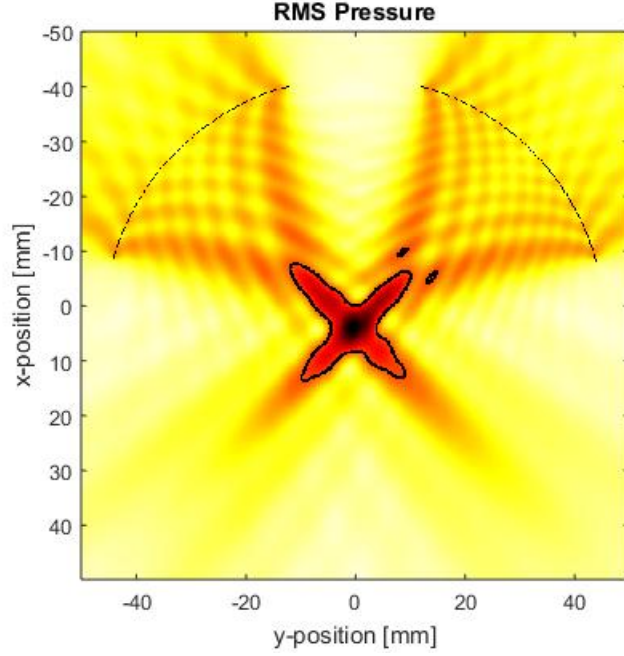


Figure 18: RMS pressure profile for $f_1 = 0.32\text{MHz}$, $f_2 = 0.25\text{MHz}$

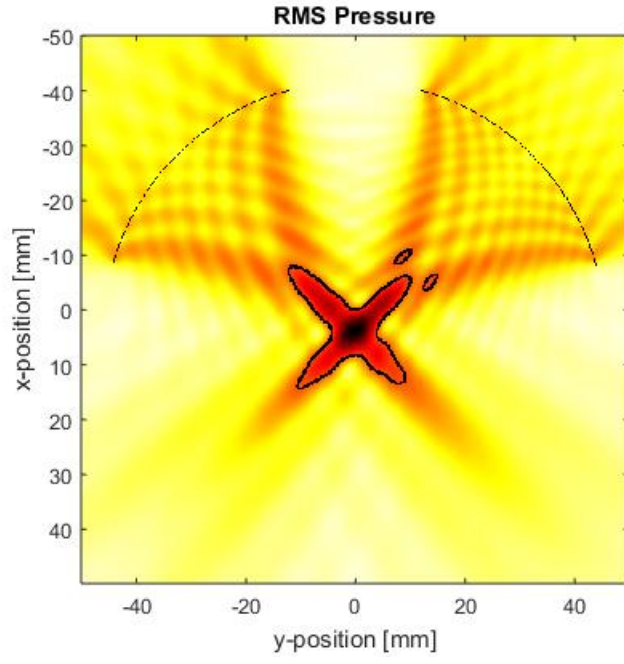


Figure 19: RMS pressure profile for $f_1 = 0.33\text{MHz}$, $f_2 = 0.25\text{MHz}$

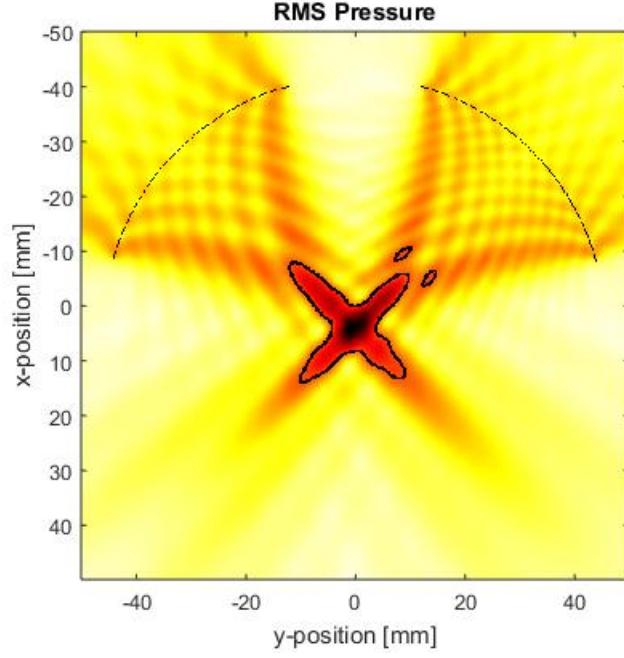


Figure 20: RMS pressure profile for $f_1 = 0.34\text{MHz}$, $f_2 = 0.25\text{MHz}$

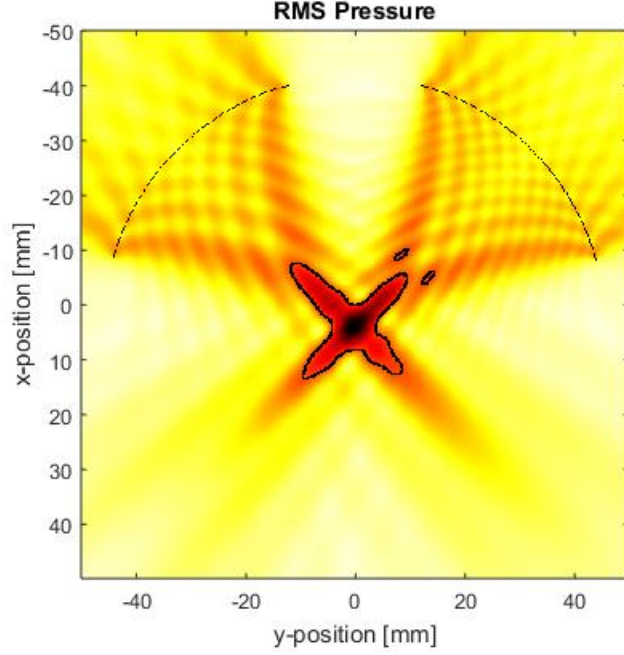


Figure 21: RMS pressure profile for $f_1 = 0.35\text{MHz}$, $f_2 = 0.25\text{MHz}$

3.2 FWHM for different frequencies

Another informative metric can be the FWHM of the profile. However, this is more useful for pressure profiles that are approximately Gaussian. The method I used for finding the points with half maximum pressure returns coordinates for all points, not just those around the central maximum. This is remediable, but the profiles remain non-circulate. The FWHM of the distributions can easily be calculated from the coordinates (x_{HM}, y_{HM}) by first calculating the coordinate of the centre of the HM points (x_{HMc}, y_{HMc}) :

$$x_{HMc} = \frac{1}{N} \sum_{i=1}^N x_{HM_i} \cdot dx, \quad y_{HMc} = \frac{1}{N} \sum_{i=1}^N y_{HM_i} \cdot dy \quad (23)$$

where N is the number of HM points. We can calculate the average distance d of the HM points from the HM centre using:

$$d = \frac{1}{N} \sum_{i=1}^N \sqrt{(x_{HM_i} - x_{HMc})^2 + (y_{HM_i} - y_{HMc})^2} \cdot dx dy \quad (24)$$

The FWHM is then approximately equal to two times the average distance between an HM point and the centre of the HM point distribution. For HM distributions that are highly non-Gaussian, then there is little purpose in calling it the FWHM - it's simply the average width of the half-maximum RMS pressure profile. Despite this, I'll continue calling it FWHM for the time being. The FWHM is shown for $200\text{kHz} \leq f_1 \leq 300\text{kHz}$ in Figure 3.2.

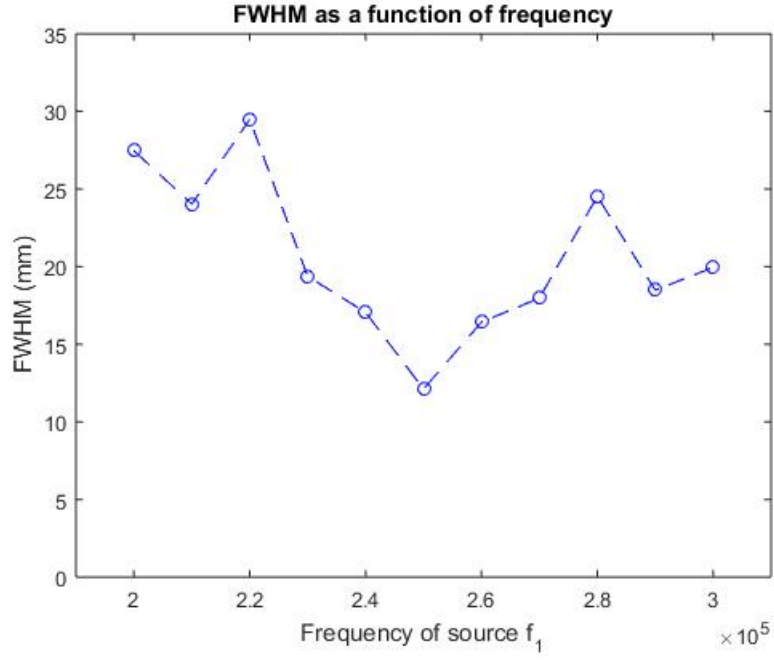


Figure 22: The FWHM of the RMS pressure distribution for $200\text{kHz} \leq f_1 \leq 300\text{kHz}$, $f_2 = 250\text{kHz}$.

3.3 Centre of HM profile

I've included this for curiosity's sake. Here I plot the centre of the FWHM profile, for $200\text{kHz} \leq f_1 \leq 300\text{kHz}$.

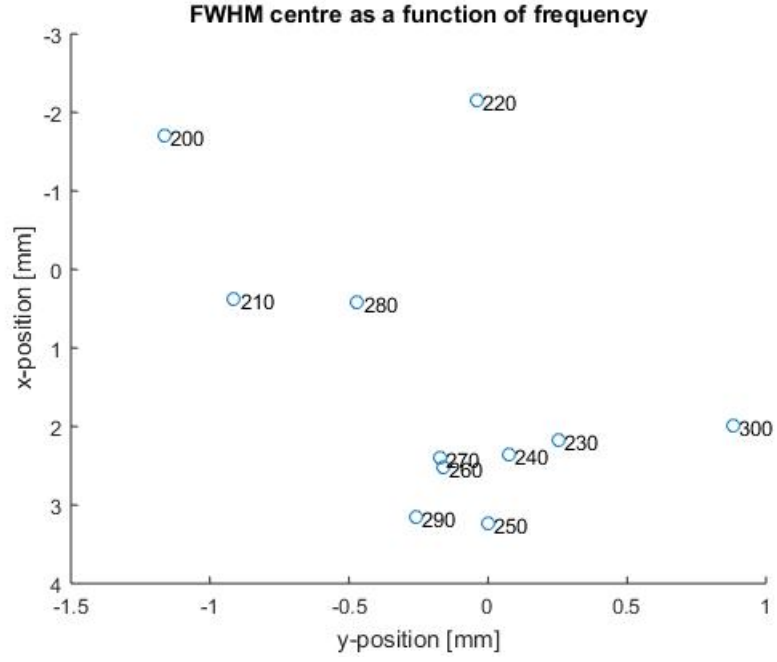


Figure 23: The coordinates of the centre of the FWHM profile of the RMS pressure distribution for $200\text{kHz} \leq f_1 \leq 300\text{kHz}$, $f_2 = 250\text{kHz}$.

3.4 Maximum RMS Pressure

We are also interested in the location of the maximum RMS intensity for different frequencies. These are shown in the following Figure 3.4.

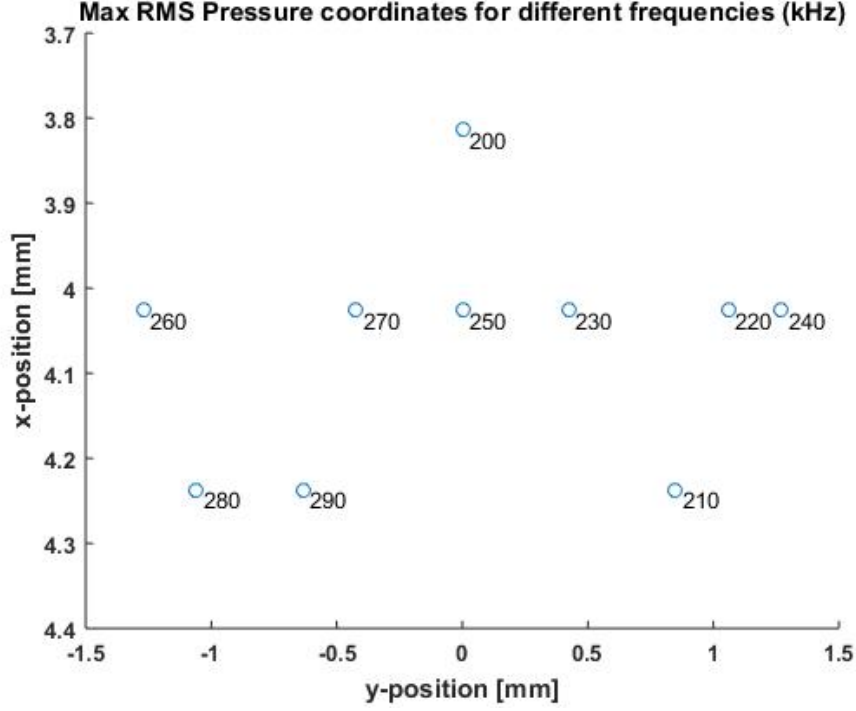


Figure 24: The Maximum RMS pressure location for $200\text{kHz} \leq f_1 \leq 300\text{kHz}$.

There does not appear to be any pattern in the location of the maximum RMS pressure coordinates. In the x-dimension, the maxima are confined to within three computational grid points, approximately +4mm away from the focal point of the independent transducers. In the y-dimension, the maxima remain closely clustered around the focal point. Generally, the maximum RMS pressure is much more highly clustered than the FWHM centre.

4 System 2: Adding Inclusions

The next step to increasing the complexity of the simulation is to add an inclusion near the focal point of the two transducers. The acoustic properties that k-wave includes are the sound speed within the medium, the ambient density distribution within the medium, a nonlinearity parameter, the power law absorption prefactor α_0 , and the power law absorption exponent y , where the power law is:

$$\alpha(f) = \alpha_0 \omega^y, \quad \omega = 2\pi f \quad (25)$$

The simulation package, k-wave, doesn't include all non-linear effects, but does include two additional non-linear terms to attempt to account for all non-linear behaviour. These terms are defined as BonA in k-wave, where A and B are the first and second terms in the Taylor series expansion of the relation between the materials pressure and density.

All of these variables can be set as spatially heterogeneous in k-wave. In order to make an accurate simulation, I will need the acoustic properties of the

medium I'll be simulating - namely water, bone, fat, nerve tissue, etc. Some of these are available in "Physical Properties of Tissue", a reference book by Francis A. Duck, and referenced by Chris Diederich in his interstitial spine simulation work [2].

For this simulation, it will also be important to be able to account for shear wave propagation. Simulation results from [3]. Luckily, there is the option to use an updated file from k-wave called PSTDELASTIC2D that allows for the separation of the compressional and shear components of the ultrasound wave. The details of the algorithm used for the propagation of shear waves in elastic media are described in full in their paper 'Modelling Elastic Wave Propagation Using the k-Wave MATLAB Toolbox' [4].

In order to understand the effect of shear wave propagation in a bone, I built another simulation, starting from the Snell's law example. In this simulation I use an inclusion centred near the focal point of the two transducers such that the ultrasound waves intersect at the proximal side of the inclusion. I set the radius of the circular inclusion to 1cm, and set the compressional speed of sound to be $v_P = 2820\text{m/s}$, the shear speed of sound to $v_S = 1500\text{m/s}$, the compressional alpha factor to $\alpha_P = 9$, and the shear alpha factor to $\alpha_S = 20$. In the rest of the simulation medium then I use $v_P = 1580\text{m/s}$, $v_s = 0\text{m/s}$, $\alpha_P = 0.57$, and $\alpha_S = 0$. I'm not sure if I should be setting α_S to zero, but since there should not be any shear waves propagating through the non-bone medium, then it should be a reasonable input. The setup for this simulation is shown in Figure ??

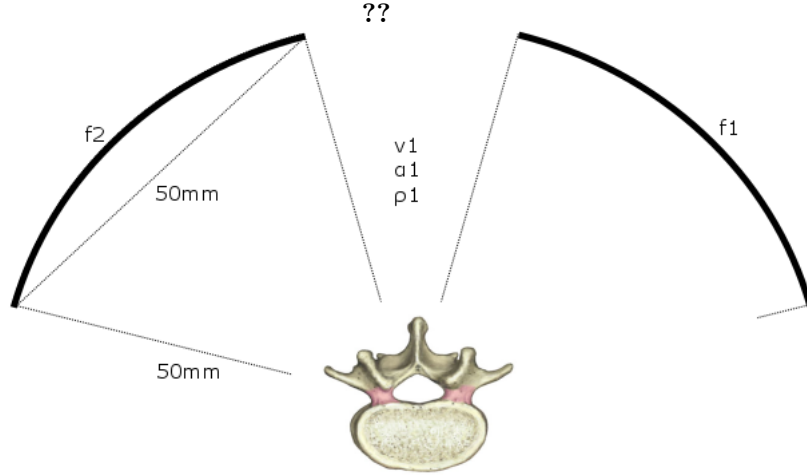


Figure 25: An inclusion is added to the system, with the same acoustic properties as those used by [3].

The code is set up to run the fluid simulation first, and then run the elastic simulation after to allow for comparison between the two models. The results of the simulation are shown in Figure 4. In this figure, the quantity plotted is the logarithm of squared particle velocity, normalized by the maximum squared particle velocity $|\mathbf{u} \cdot \mathbf{u}|/|\mathbf{u}_{max} \cdot \mathbf{u}_{max}|$. For this first test case, the frequencies of the two transducers are both 0.25MHz.

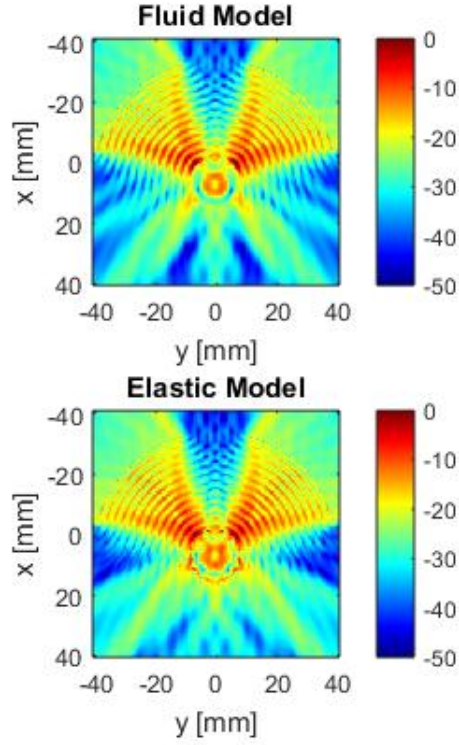
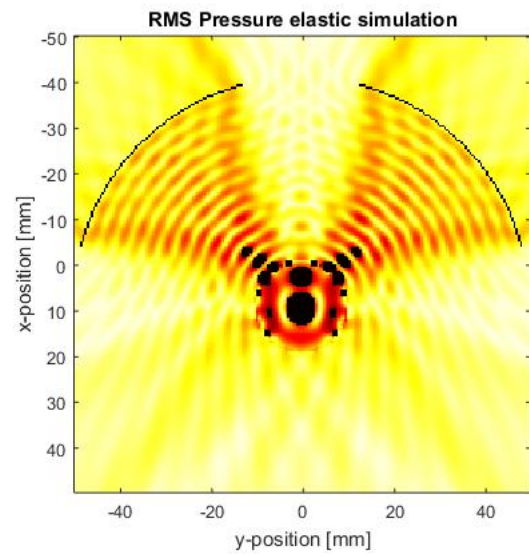
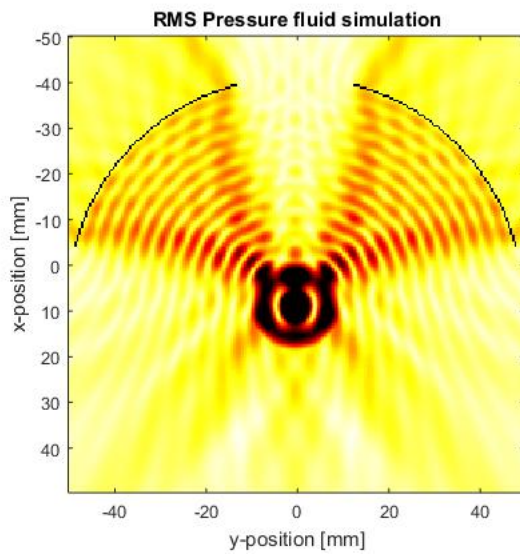
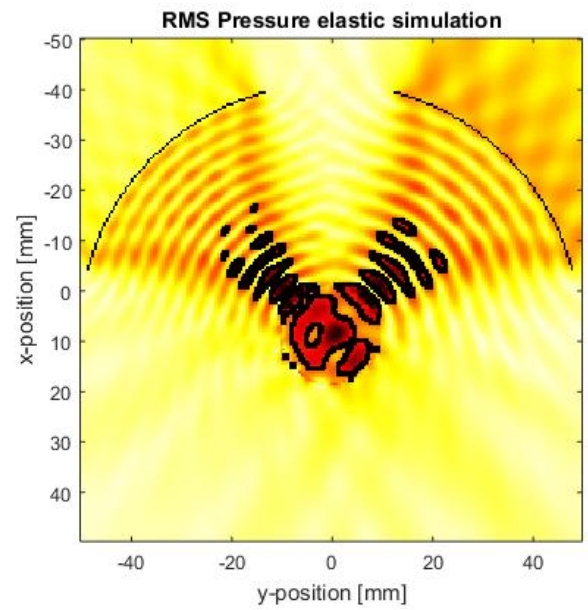
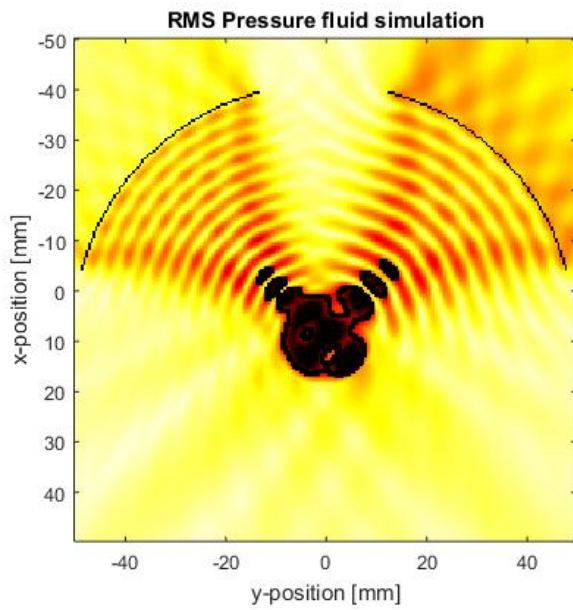


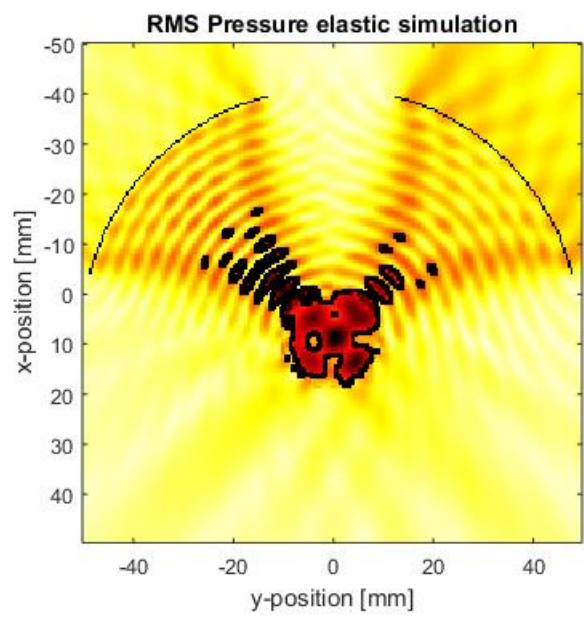
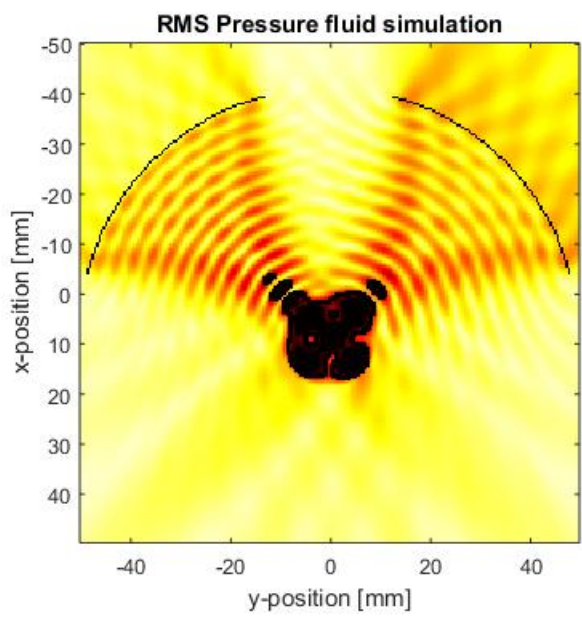
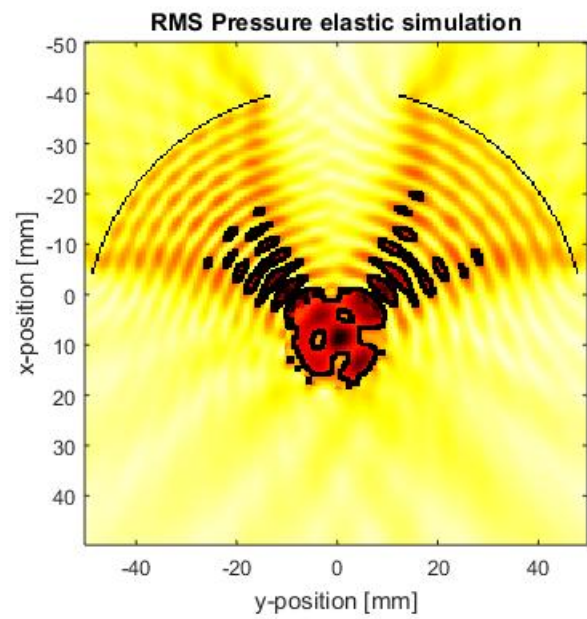
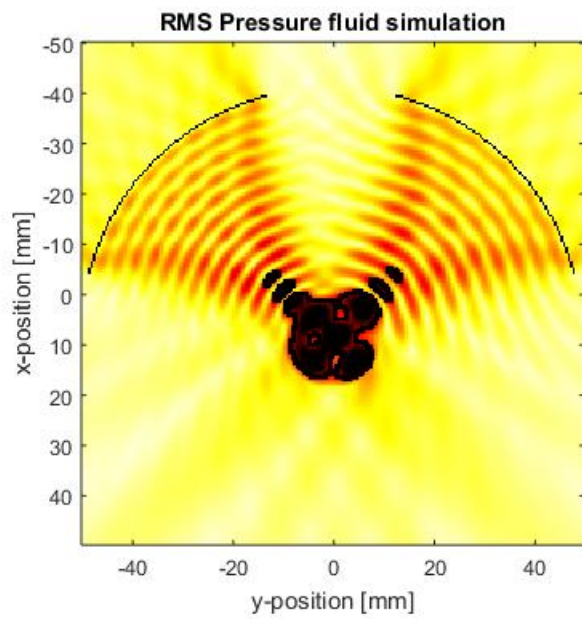
Figure 26: In this figure, the logarithm of normalized, squared particle velocity is plotted for the fluid simulation and the elastic simulation. This quantity is proportional to heat deposition, where the proportionality constants are the speed of sound in the medium, the medium density, and the absorption coefficient of the medium. This quantity, thermal deposition, is important for thermal ultrasound applications.

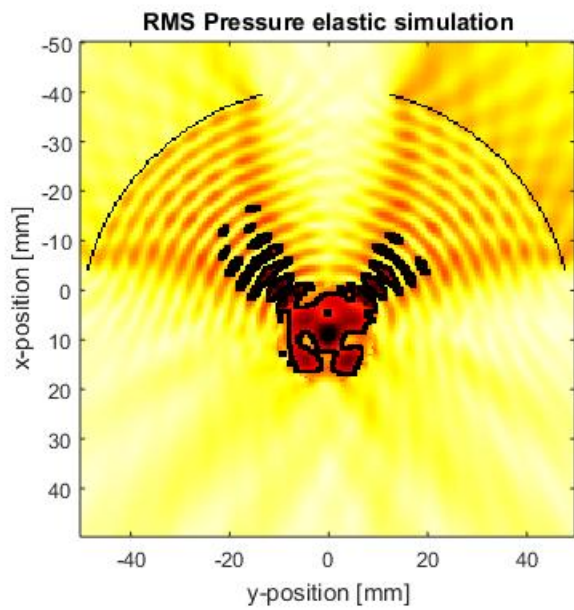
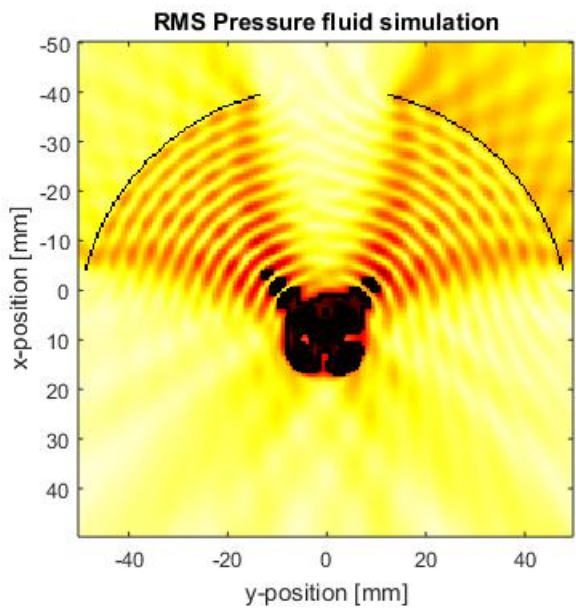
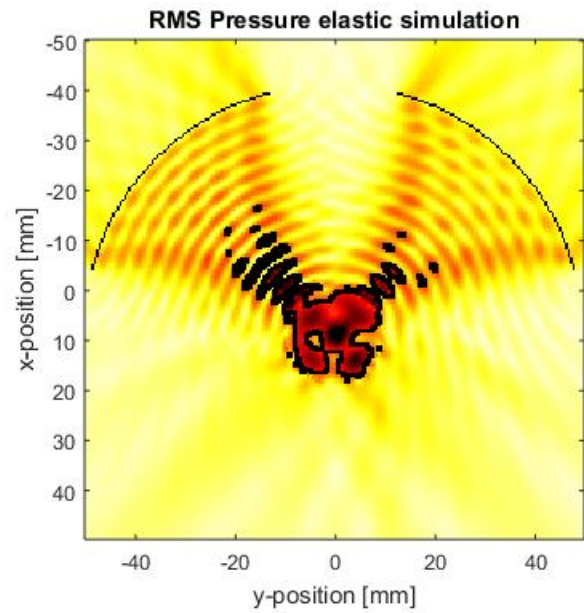
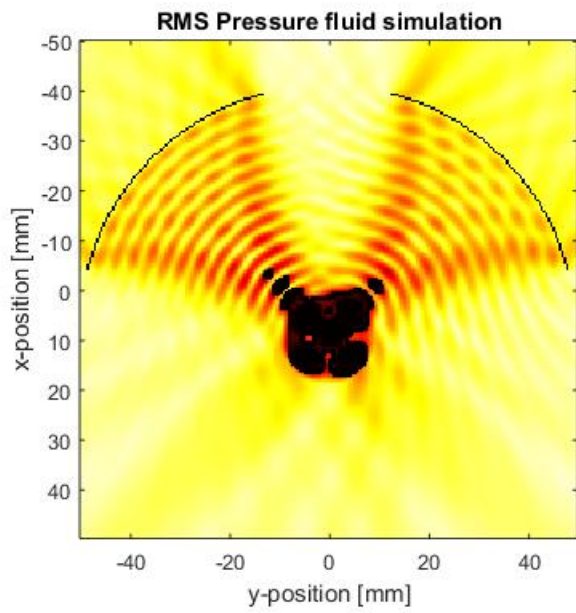
In the following figure (Figure 4) , the half-maximum contours of the RMS pressure profiles are outlined for both fluid and elastic simulations. It is somewhat difficult to see the HM lines in the figure because the pressure profiles are highly peaked.

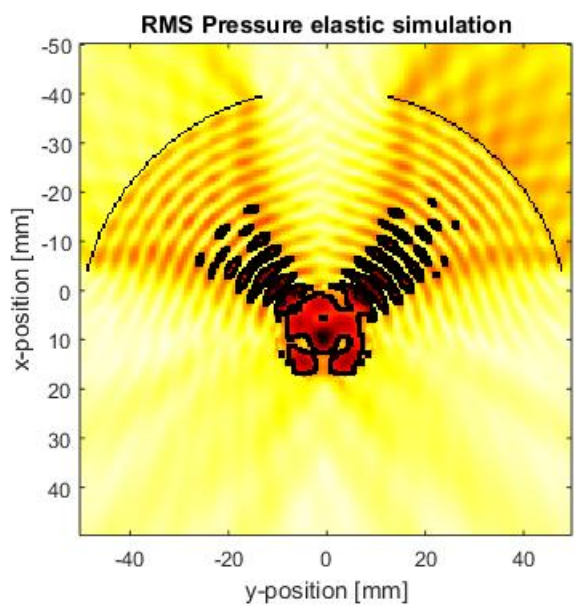
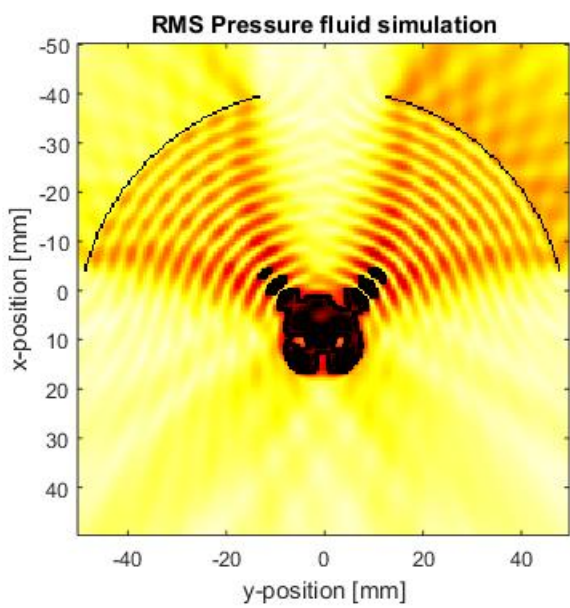
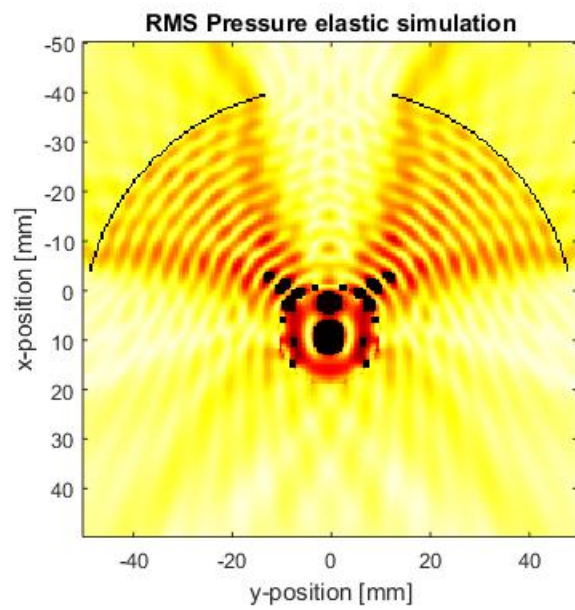
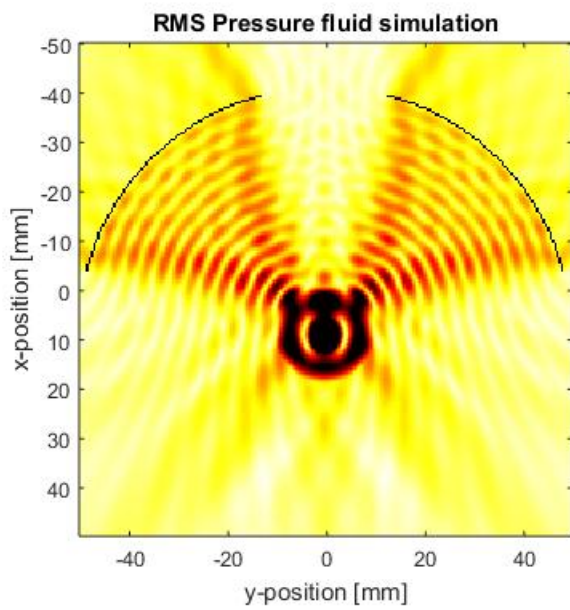


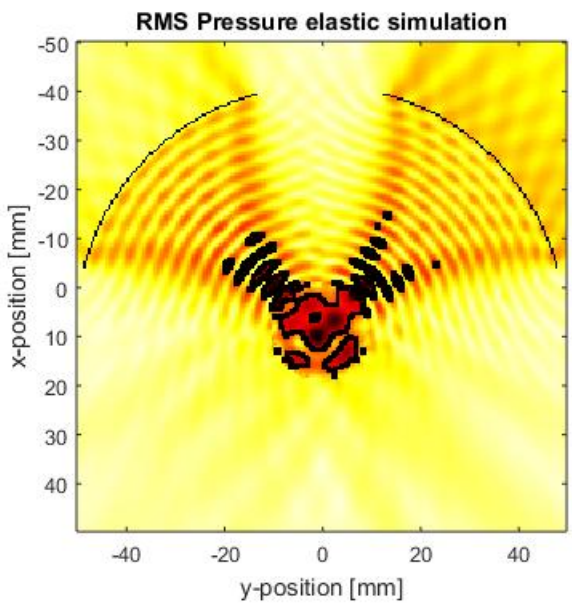
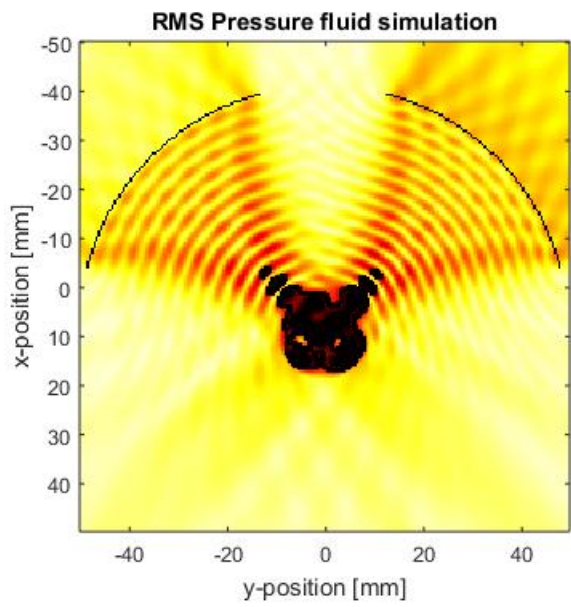
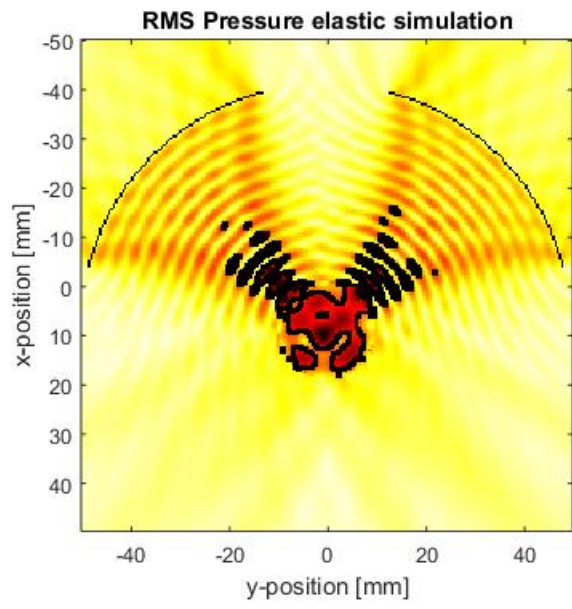
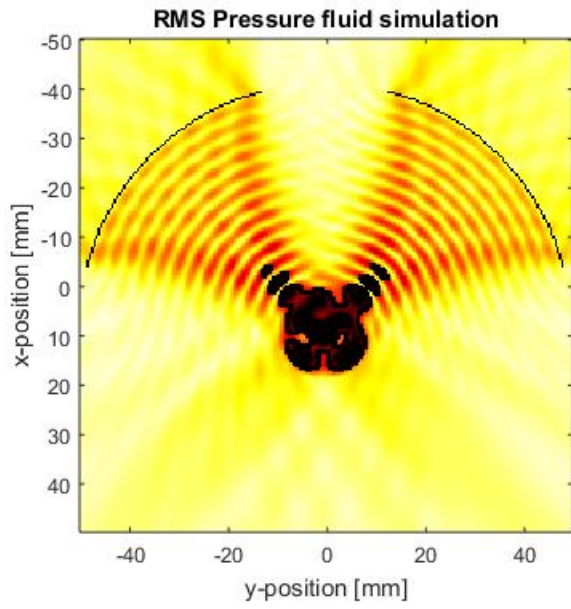
4.1 Half-Maximum Profiles

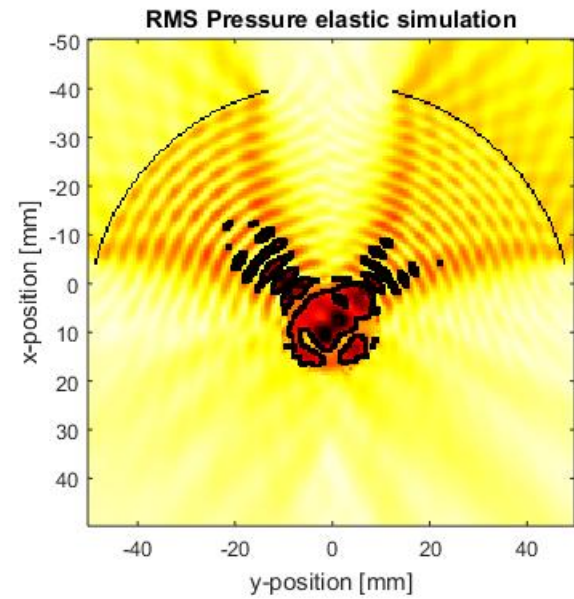
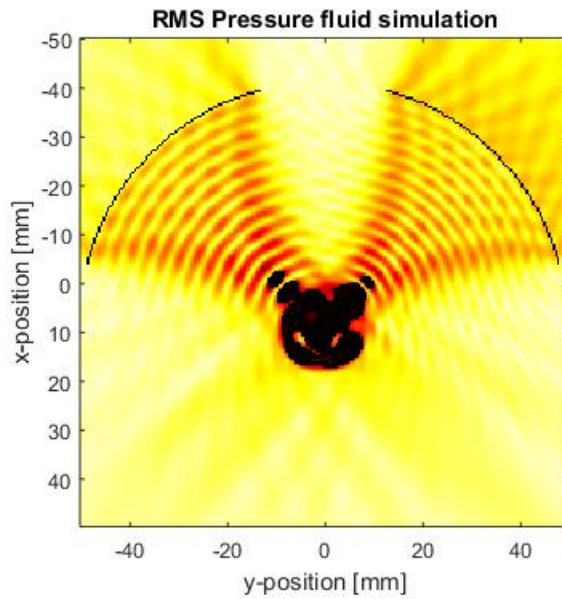
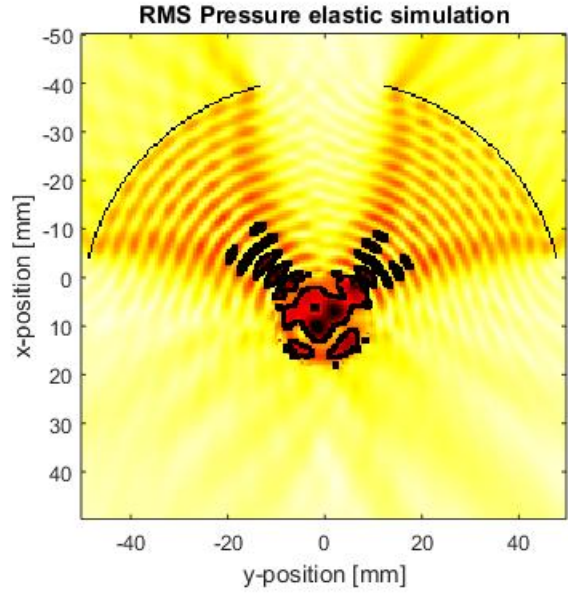
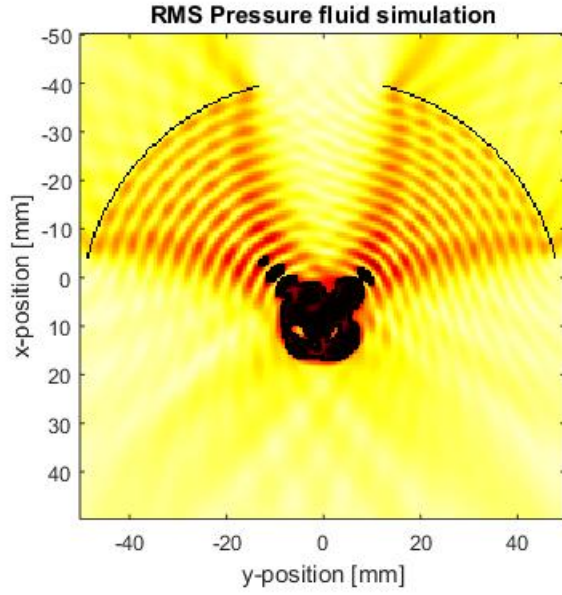












The half-maximum pressure profiles for the inclusion examples were not exactly as expected, with significant side-lobes. This, as I found out by properly reading the user manual, is because the RMS pressure profile is calculated from the entire simulation. In the simulation I've been running, I've started with a non-existent pressure profile, with the US waves then beginning to propagate

from the transducers. While this approach is suited to an application that investigated total heat deposition, it gives a bias to the initial waves and is not a good representation of the steady state system. In order to determine the characteristics of the ‘steady state system’, then we need to being the calculations of the time-averaged quantities once the US waves have propagated to the furthest points of the system.

This can be modified by setting the value `sensor.record_start_index` to the time at which the US field will have reached the furthest point in the computational box.

5 System 3: 2D vertebrae shaped inclusion

The eventual goal of this code is to produce a simulation of ultrasound interacting with a vertebrae. We start with 2D simulations to reduce the computational overhead, and plan to progress to three dimensional simulations. In this simulation, we build the environment by importing an image, rather than building the inclusion using one of the in-house functions. I found a simple image of a vertebrae online (Vertebra), and then modified it to remove colour, mark-ups, and to allow for the placement of the vertebrae near the focal point of the two transducers. The image of the vertebrae and its placement used for this system is shown in the following figure 5.

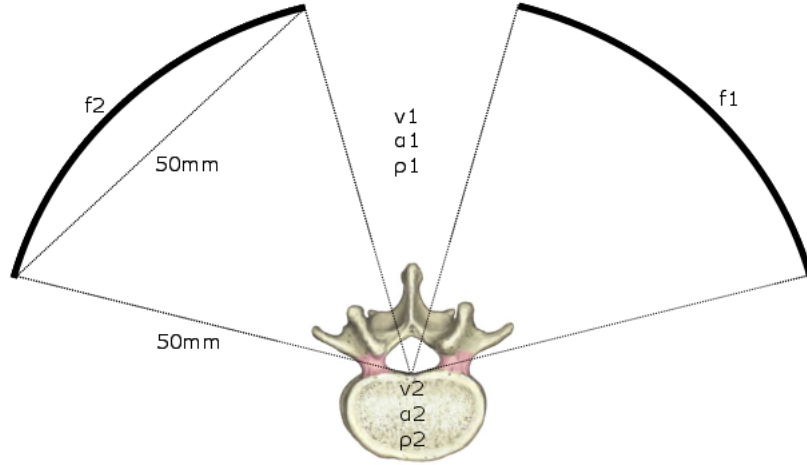


Figure 27: I used an online image I found to construct the vertebrae, and placed the vertebrae approximately at the focus of the transducers.

The image of the vertebra was binarized using the matlab function `im2bw`, where white (zero) represents water and black (one) represents bone, in order to use the image of the vertebrae to set the properties of the medium. The `im2bw` function uses a cut-off to choose whether a point is assigned as 0 (water) or 1. (bone) This cut-off may result in the erroneous assignment of points within the vertebrae as 0 or points on the exterior of the vertebrae as 1. The image must also be resized such that there is one binary grid point per computational point in the simulation ‘medium’. As explained in [5, 6], the usage of

cartesian grids to represent irregular boundaries can lead to a ‘staircase’ effect, where a boundary that is not aligned with a cartesian axis becomes irregular. However, these methods use real space calculations whereas the pseudospectral method supposedly only requires two grid points per wavelength, or four points per wavelength for inhomogeneous media. This irregularity in turn results in unwanted diffraction, and subsequently the simulation is no longer accurate. I’ve naively used the binarizing method described above, and sent this medium through both fluid and elastic simulations. The root-mean-square results are shown in the following figure 5.

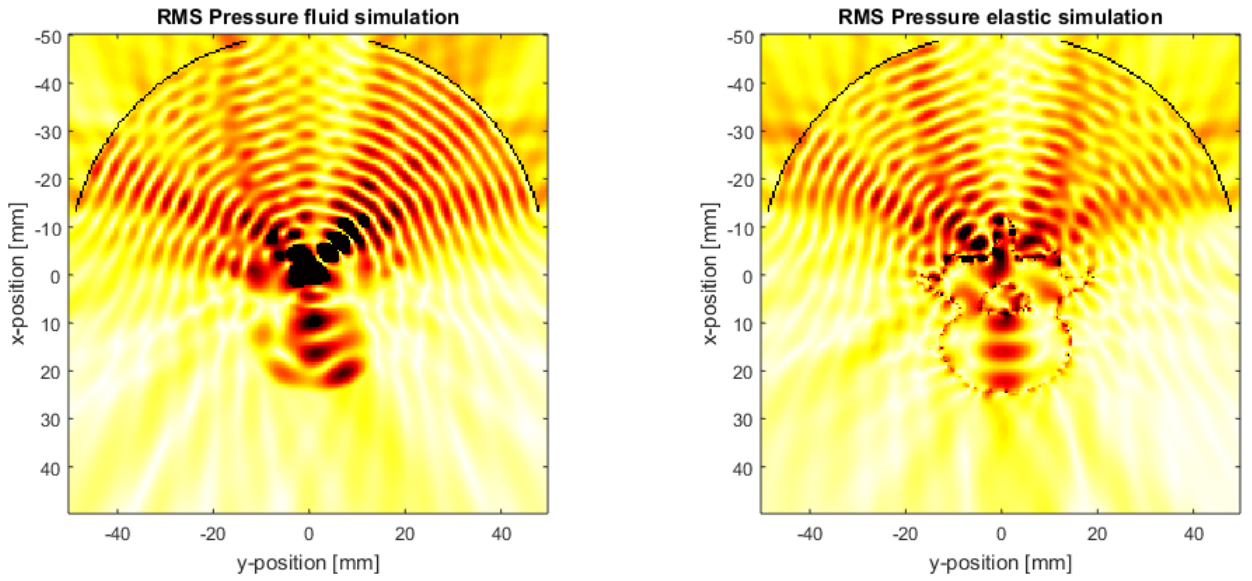


Figure 28: K-wave simulation results using a binary mask of an image of a vertebra. The results from the elastic simulation show that the irregular boundary of the vertebra gives erroneous diffraction, absorption, etc. from the inclusion.

References

- [1] R. E. Mickens, *Nonstandard finite difference models of differential equations*. world scientific, 1993.
- [2] F. Duck, “Physical properties of tissue: A comprehensive reference book (academic, london),” 1990.
- [3] B. E. Treeby and T. Saratoon, “The contribution of shear wave absorption to ultrasound heating in bones: Coupled elastic and thermal modeling,” in *Ultrasonics Symposium (IUS), 2015 IEEE International*, pp. 1–4, IEEE, 2015.
- [4] B. E. Treeby, J. Jaros, D. Rohrbach, and B. Cox, “Modelling elastic wave propagation using the k-wave matlab toolbox,” in *2014 IEEE International Ultrasonics Symposium*, pp. 146–149, IEEE, 2014.
- [5] F. Muir, J. Dellinger, J. Etgen, and D. Nichols, “Modeling elastic fields across irregular boundaries,” *Geophysics*, vol. 57, no. 9, pp. 1189–1193, 1992.
- [6] B. Vafaeian, M. El-Rich, T. El-Bialy, and S. Adeeb, “The finite element method for micro-scale modeling of ultrasound propagation in cancellous bone,” *Ultrasonics*, vol. 54, no. 6, pp. 1663–1676, 2014.